Synthesis of Composite Adsorbent from Calcium Carbonate and *Cocos Nucifera* Carbon Powder Crosslinked with Biopolymer Matrix

M A Kamaruddin[1,2]**, M M A Bakri**[2]**, F A Norashiddin**[1]**, M H Zawawi**[3] **and M R R A Zainol**[4]

[1]Environmental Technology Division, School of Industrial Technology, Universiti Sains Malaysia, 11800 Penang, Malaysia
[2]Center of Excellence Geopolymer & Green Technology (CEGeoGTech), Universiti Malaysia Perlis, Perlis, Malaysia
[3]College of Engineering, Universiti Tenaga Nasional, Jalan Serdang, Seksyen 11, Selangor, 43650 Bandar Baru Bangi, Malaysia
[4]School of Civil Engineering, Universiti Sains Malaysia, Engineering Campus, 14300 Nibong Tebal, Penang, Malaysia

anuarkamaruddin@usm.my

Abstract. The use of coconut shell based adsorbent for removing various pollutants from wastewater offers attractive advantages such as exceptional adsorption capacity with larger surface area, low-cost and biocompatibility for a wide range of pollutants. The same goes for calcium carbonate based adsorbent, which provides better removal for metals ions through precipitation method. In fact, recycling of waste material is considered environmentally preferable and is supported by public opinion and government policy. However, because of unit operations mechanisms and effectiveness are different to one another in downstream process, it is quite difficult to provide good adsorbent that exhibits dual attributes of hydrophobic and hydrophilic characters. This paper provides brief process for sintering of composite adsorbent for separation and purification of industrial wastewater application. Characterization was performed by physical and chemical approach. Results prove that the inclusion of biopolymer as composite binder improved mechanical properties of the composite adsorbent.

1. Introduction
Generally, activated carbon has been the adsorbent of choice rather than the others because of their physical and/or chemical properties that can easily be tailored in order to optimize their performance [1]. Activated carbon has a very porous structure with a large internal surface area ranging from 500 to 2000 m^2/g that makes it a good adsorbent in the adsorption process [2]. Broad application of activated carbon is due to its chemical and mechanical stability, high degree of surface reactivity and high adsorption capacity [3]. Common types of activated carbon are granular (GAC) and powdered (PAC) form. Granular activated carbon is produced from hard materials that may be used to remove pollutants from wastewater with no requirement to separate the activated carbon from bulk fluid.

Large particle size of GAC presents a smaller surface area thus suitable for diffusion (gas and odor) purpose. Meanwhile, PACs may be obtained from crushed ground carbon particles that pass designated sieve aperture. Typical size of PAC granules are less than 1.0 mm with average diameters of 0.15 to 0.25 mm [4].

Despite overwhelming anticipation in textile wastewater treatment, the biggest barrier of commercial activated carbon is the prohibitive cost and difficulty associated with regeneration [5, 6]. Moreover, large scale application for activated carbon will only raise the operational cost of a treatment plant due to the expensive cost of activated carbon over the years (M. A. Kamaruddin, Yusoff, & Ahmad, 2011). Therefore, the drawbacks of commercial activated carbon have resulted in a growing research interest searching for low-cost alternative precursors for activated carbon as cheaper and renewable are the trends among scientists in the recent years [7].

In the field of wastewater treatment, limestone is commonly employed to remove certain types of heavy metals such as manganese; as discussed by Aziz and Smith [8]. This study attempted to use limestone particles to remove manganese from water containing 53.9% $CaCO_3$ and 5.2% $MgCO_3$, gravel, crushed bricks or without solid media at different pH values. They found that at final pH value of 8.5, the removal of Mn using limestone, crushed bricks, gravel, aeration and settlement without solid media were 95%, 82%, 60% and less than 15% respectively, in exploring the capabilities of limestone in purifying wastewater.

Although abundant literature data for the application of coconut shell based activated carbon and limestone particle in wastewater treatment, there are still gap of knowledge to be further explored such as enhancement of adsorption capacity through modification of *Coco Nurfira* carbon (CSAC) and calcium carbonate powder (LP) with the presence of sodium alginate as biopolymer binder. In fact, there is very limited information on the assessment of sodium alginate composite based adsorbent for in terms of their physical and chemical characteristics. Thus, this study attempts to provide brief supporting data for the potential of composite preparation by the combination between hydrophobic and hydrophilic precursors.

2. Materials and Methods
2.1 Composite preparation
Briefly, the composite was prepared based on [9, 10]. The composite adsorbent preparation involved several physical and mechanical procedures and small modification was adapted in order to suit the different characteristics of *Coco Nufira* carbon (CSAC) and calcium carbonate powder (LP). First, known amount of CSAC and LP was introduced into 500 mL beaker. A known volume of distilled water was then added and stirred with mechanical stirrer (Ika, Germany) for 15 minutes with 50 rpm speed.

Next, the beaker was heated to 80 °C on a hot plate and alginate powder was slowly added into the beaker. This process was maintained for 15 minutes until a homogeneous condition between CSAC, LP and alginate was reached. The mixture was then transferred via peristaltic pump into the beads injector. Figure 1 illustrates the schematic diagram of the experimental set up. The mixture was then extruded from the injector by controlling the opening of control valve. Finally, the release composite beads were immersed in $CaCl_2$ solution for 12 hours to achieve hardened beads. Figure 1 illustrates the schematic diagram of the experimental set up.
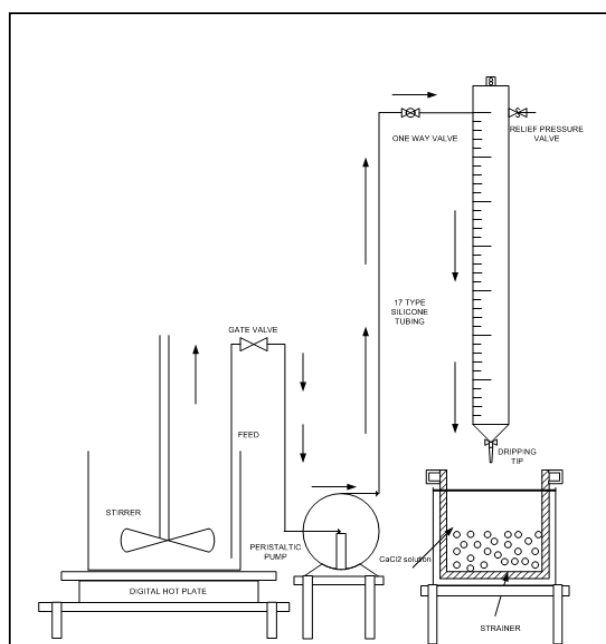
Figure 1. Schematic flow of composite preparation

2.2 Physical and Chemical Characteristics Analysis

X-ray powder diffraction (XRD)

X-ray powder diffraction (XRD) was used to support the SEM image attained. XRD is the most common technique used to determine the mineral composition of composite adsorbent that exists in the crystalline state. The equipment used was D2 Phase (Bruker). It is based on Brag Equation as follows:

$$\eta\lambda = 2d\sin\theta \tag{1}$$

Thermogravimetry Analysis

Thermal analysis or Thermogravimetry Analysis (TGA) was carried out using TGA Analyzer (DTG 60 H Shimadzu, Japan). Principally, 5 mg of sample was loaded into a crimp cell whereby the pan holder was used to minimize the potential reaction with the sample. The furnace chamber was then raised and degassed for several minutes. During inert atmosphere exertion in the chamber, a small amount of sample was heated up to 110 °C for complete dehydration and followed by decomposition at 850 °C for 7 minutes to determine volatile matters. Oxidizing state was achieved once the sample was cooled down to 600 °C and this process was maintained until there was no change in the weight of sample.

Fourier Transform Infrared (FTIR) Spectroscope

An FTIR transmission spectrum of the sample was carried out by using an FTIR spectroscope (Model Perkin Elmer 2000, USA). The purpose of FTIR measurement is to study the surface chemistry of the raw materials and the composite adsorbent by exploring the functional groups present in the sample surfaces. Prior to the analysis, the sample was ground into a fine form that can pass a 75 μm sieve aperture and dried at 110 °C for 12 hours. Next, the solid sample was mixed with 400 mg of potassium bromide (KBr) using impact mortar and pestle. A translucent round disk of 12.7 mm internal diameter and 1 mm thickness was retrieved by using a bench press with 8 tons of pressure. The translucent disk was then placed into the infrared spectrometer. Finally, with the aid of software (Spectrum version

5.0.2) in the FTIR spectroscope system, the wave number in the range of 400-4000 cm^{-1} was eventually recorded.

Results and Discussions

X-ray Diffraction (XRD)

Figure 2 illustrates important peaks that emerged from the XRD analysis were carbon nitride 84.1%, calcium peroxide (6.4%), iron nitride (2.8%), potassium oxide (5.4%) and magnesium zinc (1.3%). These peaks were observed in the range of 24° to 48°. However, except the peak intensity, the presence of AG ($Na_2C_6H_7O_6$) was not observed due to the weakened condition after forming within the composite adsorbent [11]. In the amorphous phase, normally X-rays will be scattered in many directions leading to a large bump distributed in a wide range (2 Theta) instead of high intensity narrower peaks. In this case, plenty of remotely narrow peaks emerged which suggested the degree of amorphous and large particle size that could be observed from Figure 2 (b).

The tricarbon tetranitride peak was observed at 30° with 41.4% intensity. Meanwhile, the formation of hydrogen (28.7%) element suggested sufficient paths for oxygen bonding during the adsorption process. This reaction could initiate hydrogen bonding with carboxylic, hydroxyl as well as amines groups for metal sorption, respectively. Overall, the composite adsorbent suggested the amorphous condition rather than crystalline because of the interference of irregular base line with noise and pulsed shape being the highly noisy line is the highly amorphous phase as manifested from Figure 2.
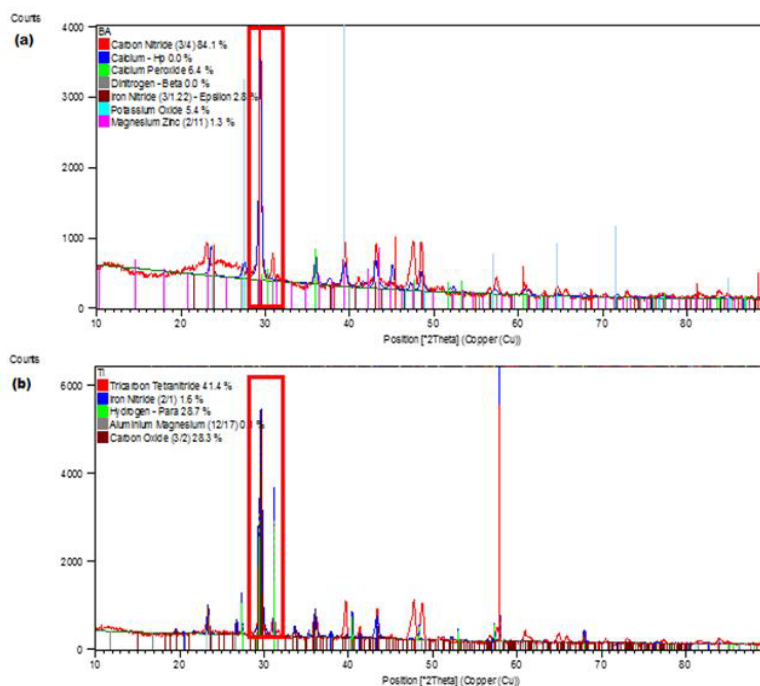

Figure 2. XRD patterns of (a) Composite adsorbent before adsorption and (b): composite adsorbent after adsorption

Thermogravimetry Analysis

Figure 3 shows the TGA plot of the composite adsorbent before and after adsorption process. As shown in the figure, gradual weight loss occurred for the dried composite adsorbent during heating between 0-200 °C, which was attributed by moisture loss (5.01%). The next heating step to 400 °C

caused a weight loss of 27.71% of initial dry mass, indicating volatile matter combustion [12]. Further increased heating rate to 600 °C caused significant loss of the initial dry sample to 79.30% which largely represented by the fixed carbon. Finally, the ash content showed 7.96% from total weight loss. However, the transition of weight loss for the spent composite adsorbent after adsorption indicates slight changes in terms of weight %. From the figure, only 1.45% of moisture loss can be observed during thermal analysis. This condition was due to the oversaturated condition of the composite adsorbent. In fact, this phenomenon proved the water bearing capacity of the adsorbent with the presence of sodium alginate as the core binder [13]. Further increased heating from 200 to 600 °C led to reduction weight loss of 14.36 and 62.88% than original weight of the sample which represent the volatile matter and fixed carbon contents. The weight loss of the composite adsorbent as shown in the figure suggested the matrix decomposition of carbon that is rich with fixed carbon and ash as partial constituents in the adsorbent [14].
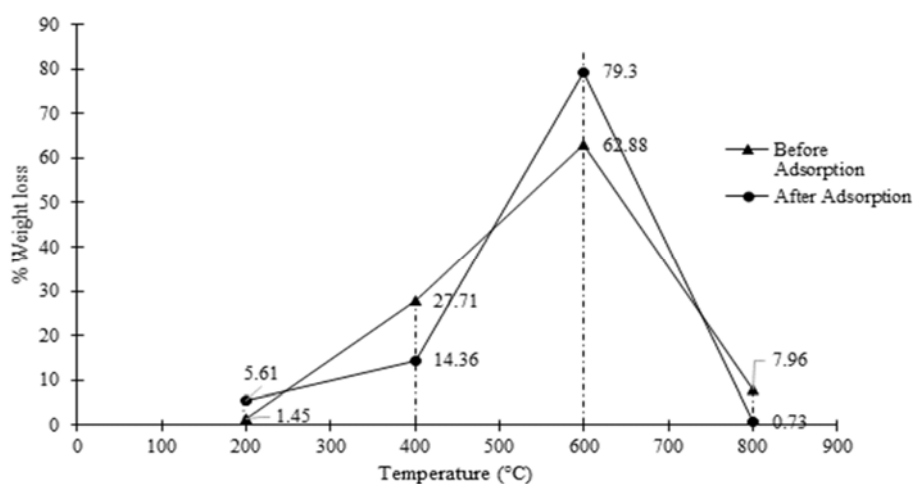

Figure 3. TGA of composite before and after trial adsorption

Fourier Transformation Infrared (FTIR) Spectroscope
The adsorption characteristics of a composite adsorbent are also influenced by the surface functional groups, which can be determined from the Fourier Transform Infrared (FTIR) spectroscopy analysis. Figure 4 illustrates the FTIR spectrums of the composite adsorbent before and after undergoing adsorption process. Based on FTIR spectrums (Figures 4.19 (a) and (b)), the surface chemistry of the composite adsorbent before and after adsorption of the precursors showed some differences due to the modification of many functional groups of the precursors during the gelation process. In fact, the most dominant peak observed were C≡N stretching nitriles of 2358 cm^{-1} that conformed to significant presence of alginate as the binding agent for the precursors (Figure 4.9 (a)).

The FTIR spectrums also revealed that the functional groups in the precursors such as CSAC and alginate (AG) have been shifted to C=O stretching alpha (1726 cm^{-1}), which belongs to unsaturated esters. This functional group also indicated that the shifted spectrums from aliphatic amines to C=O stretching provides the exchange path during the adsorption course. In fact, those medium peaks that have been detected from the precursors were mostly belonging to general carbonyl groups, in which stretching were from 1665 to 1769 cm^{-1}. Next, another significant peak observed for the composite adsorbent before the adsorption was at band 1025 cm^{-1}. The spectrum belongs to aliphatic amines group that stretch from C-N, which implied important absorption bands for grafting purpose of alginate in the gelation process.

Figure 4 (b) shows the FTIR spectrums of the composite adsorbent after the adsorption process. From the figure, there was significant H stretching vibrations of hydroxyl functional groups including hydrogen bonding, which was detected at a bandwidth of 3409 cm^{-1}. The location of the detected hydrogen-bonded O-H group is usually in the range of 3200–3750 cm^{-1} for alcohols and phenols and related to adsorbed water [15]. However, the disappeared medium C=O stretching bond was found shifted to 1408 cm-1 and belong to C–C stretch aromatics rings. The shift to lower wave numbers in comparison with AG samples explained the interaction of the regular long chain with the sodium ions [16]. Table 1 summarizes detected bandwidth of composite adsorbent in this work with respect to previous works.
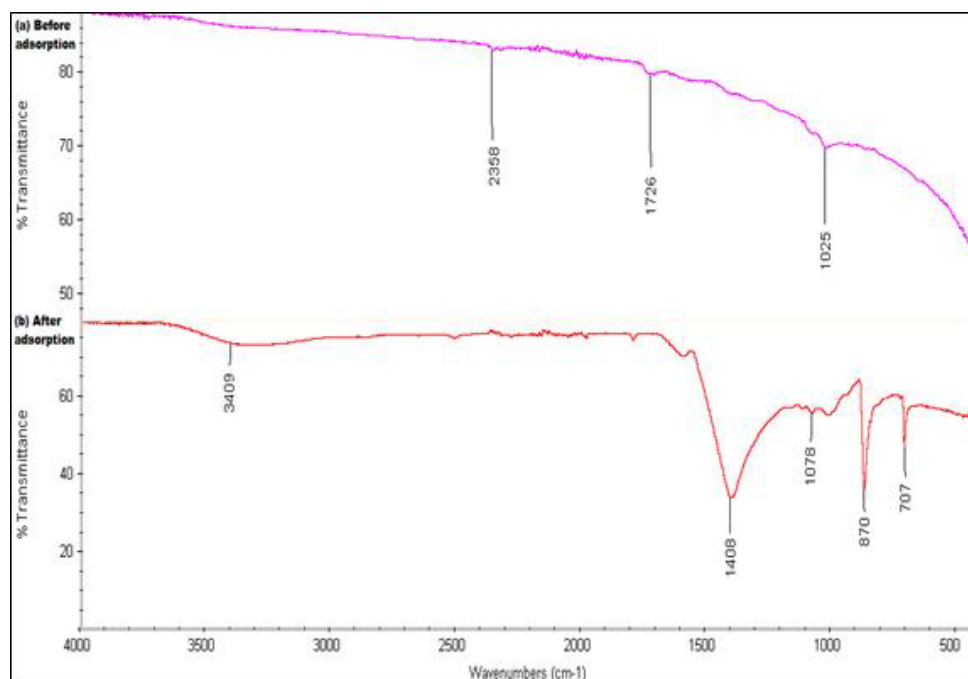

Figure 4. FTIR spectrums of composite adsorbent (a) before and (b) after adsorption

Conclusions
Based on the preliminary analysis, the results have demonstrated the successful synthesis of composite from hydrophobic and hydrophilic conjugates through biopolymerization technique. From the XRD analysis, the composite adsorbent was categorized as having amorphous structure, thereby plenty of narrower peaks were detected in a wide range of 2 theta. TGA analysis has shown that water bearing capacity as a result from preparation condition was responsible for the high moisture content of the composite. FTIR results indicated the presence of functional groups such as hydroxyl, carbonyl and alkyl on the surfaces of the composite adsorbent prepared. Further studies for the effectiveness of the composite shall be expanded in near future.

References

[1] Mezohegyi, G., van der Zee, F. P., Font, J., Fortuny, A., & Fabregat, A. (2012). Towards advanced aqueous dye removal processes: a short review on the versatile role of activated carbon. *Journal of Environmental Management, 102*, 148-164.

[2] Ribas, M. C., Adebayo, M. A., Prola, L. D., Lima, E. C., Cataluña, R., Feris, L. A., . . . Calvete, T. (2014). Comparison of a homemade cocoa shell activated carbon with commercial activated carbon for the removal of reactive violet 5 dye from aqueous solutions. *Chemical Engineering Journal, 248*, 315-326.

[3] Trikha, R., & Sharma, B. K. (2014). Studies on factors affecting fluoride removal from water using passive system. *Journal of Environmental Chemical Engineering, 2*(1), 172-176.

[4] Salleh, M. A. M., Mahmoud, D. K., Karim, W. A. W. A., & Idris, A. (2011). Cationic and anionic dye adsorption by agricultural solid wastes: A comprehensive review. *Desalination, 280*(1), 1-13.

[5] Hung, Y. T., Aziz, H. A., Amr, S. S. A., Yeh, R. Y. L., Liu, L. H., & Kamaruddin, M. A. (2013). Chemicals and allied products. *Water Environment Research, 85*(10), 1474-1500. doi: 10.2175/106143013X13698672322426

[6] Hung, Y. T., Aziz, H. A., Yusoff, M. S., Kamaruddin, M. A., Yeh, R. Y. L., Liu, L. H., . . . Fu, Y. P. (2015). Chemical waste and allied products. *Water Environment Research, 87*(10), 1312-1359. doi: 10.2175/106143015X14338845155822

[7] Kamaruddin, M. A., Yusoff, M. S., & Aziz, H. A. (2014). Preparation and Characterization of Alginate Beads By Drop Weight. *International Journal of Technology, 5*(2), 121-132.

[8] Aziz, H. A., & Smith, P. G. (1996). Removal of manganese from water using crushed dolomite filtration technique. *Water Research, 30*(2), 489-492.

[9] Kamaruddin, M. A., Yusoff, M. S., & Ahmad, M. A. (2011). Optimization of durian peel based activated carbon preparation conditions for ammoniacal nitrogen removal from semi-aerobic landfill leachate.

[10] Kamaruddin, M., Yusoff, M., Aziz, H., & Alrozi, R. (2017). Statistical Determination for Eco-Friendly Composite Adsorbent Preparation for the Removal of COD, Colour and Cu (II) from Textile Effluent. *Journal of Scientific & Industrial Research, 76*, 506-511.

[11] Lv, X., Jiang, G., Xue, X., Wu, D., Sheng, T., Sun, C., & Xu, X. (2013). Fe 0-Fe 3 O 4 nanocomposites embedded polyvinyl alcohol/sodium alginate beads for chromium (VI) removal. *Journal of hazardous materials, 262*, 748-758.

[12] Lemlikchi, W., Sharrock, P., Mecherri, M., Fiallo, M., & Nzihou, A. (2012). Treatment of Textile Waste Waters by Hydroxyapatite Co-Precipitation with Adsorbent Regeneration and Reuse. *Waste and biomass valorization, 3*(1), 75-79.

[13] Donati, I., & Paoletti, S. (2009). Material properties of alginates *Alginates: Biology and applications* (pp. 1-53): Springer.

[14] Shen, Y.-S., Wang, S.-L., Tzou, Y.-M., Yan, Y.-Y., & Kuan, W.-H. (2012). Removal of hexavalent Cr by coconut coir and derived chars–The effect of surface functionality. *Bioresource technology, 104*, 165-172.

[15] Ahmad, A., & Hameed, B. (2009). Reduction of COD and color of dyeing effluent from a cotton textile mill by adsorption onto bamboo-based activated carbon. *Journal of hazardous materials, 172*(2), 1538-1543.

[16] Daemi, H., & Barikani, M. (2012). Synthesis and characterization of calcium alginate nanoparticles, sodium homopolymannuronate salt and its calcium nanoparticles. *Scientia Iranica, 19*(6), 2023-2028.